

New developments in fission studies within the time-dependent density functional theory framework

Aurel Bulgac¹

¹Department of Physics, University of Washington, Seattle, WA 981965-1560, USA

Abstract. We have extended significantly the microscopic description of the fission process by examining a larger set of observables. We extract neutron and proton numbers of fission fragments, their spins and fission fragment relative orbital angular momentum and their correlations, investigate neutrons emitted at or shortly after scission, excitation energy sharing mechanism, total kinetic energy of fission fragments, and the entanglement entropy. I will present a short overview of our simulations obtained with two independent nuclear energy density functionals.

1 Introduction

Nuclear fission, which was discovered in 1939 by Hahn and Strassmann [1] and its leading microscopic mechanism was described almost immediately by Meitner and Frisch [2]. In spite of more than 80 years since a fully microscopic description of fission dynamics still eludes us. Most theoretical developments have been phenomenological, many of them making contradictory assumptions, typically not supported by a microscopic confirmation, but in the end reaching agreement with data, largely due to a large number of phenomenological parameters. There exist as well a range of microscopic approaches, based on unchecked assumptions and numerical approximation. There are only three possible avenues to follow for a fully microscopic treatment of this non-equilibrium quantum process: 1) solve the time-dependent many-body Schrödinger equation (TDSE); 2) solve the time-dependent density functional theory (TDDFT) extended to nuclear systems; 3) solve a time-dependent formulation of QCD. Solving TDSE is unfeasible, and moreover we do not know with enough accuracy the interactions between nucleons. In this respect the QCD route is even more hopeless, as it is even more complicated than solving TDSE. The only route to follow for perhaps many decades is the TDDFT and its needed extension, to which I will allude a little bit.

2 Why use Density Functional Theory?

It has been mathematically proven than TDDFT [3–8] is equivalent to the TDSE at the level of one-body density.¹

¹Nuclei, similarly to electrons, need in principle an external one-body potential for this statement to be in agreement with Hohenberg and Kohn theorem [3]. Unlike infinite systems, in case of finite nuclei one can always add a one-body square-well potential of sufficiently large diameter, which can eventually be taken to infinity, and establish thus formally the one-to-one relation between the number density and the many-body wave function.

TDDFT has the great advantage, that unlike many phenomenological approaches, is a quantum framework, but also a disadvantage, as we do not know with great accuracy its main ingredient, the nuclear energy density functional (NEDF). The quality of *ab initio* nucleon interaction approaches [9, 10] and the corresponding derived NEDFs are still of insufficient accuracy for the treatment of heavy nuclei. For the time being we will have to rely on accurate phenomenological NEDFs [11].

3 Crucial theoretical input

The crucial question in addressing a microscopic description of fission is: What are the essential ingredients without which we are doomed to fail? Surprisingly, the number of essential ingredients to describe accurately nuclear masses, charge radii and many other static properties of nuclei [11] are exactly the same which are required for the dynamic description of fission, which is a time-dependent process and intrinsically a non-equilibrium one as well.

- Nuclear surface tension and Coulomb interaction between protons. These two nuclear properties are known from Bethe-Weizsäcker mass formula, suggested by Gamow in 1930. Meitner and Frisch [2] realized that fission is driven by the competition between the surface and the Coulomb energies, and is not a tunneling process as was the prevailing attitude at the time.
- The strength of the spin-orbit interaction. In the absence of spin-orbit interaction the average masses of the heavy and light fission fragments (FFs) and the presence of the second fission isomers cannot be described [12, 13], and the most probable split will be two FFs of equal masses.
- The strength of the neutron and proton pairing. In the absence of pairing fission would be strongly hindered [14–18]. Inclusion of pairing requires an extension of DFT to superfluid systems, the time-dependent

superfluid local density approximation (TDSLDA) [19, 20] in the spirit of the Kohn-Sham LDA [4].

- Symmetry energy of symmetric nuclear matter, needed to correctly describe the N/Z composition of FFs, and to a lesser extent its density dependence.
- Saturation density and binding energy of symmetric nuclear matter, needed to correctly describe the dynamics of an incompressible fissioning liquid drop [2, 21].

As in the case of the many-body Schrödinger equation, where we still do not know with sufficient accuracy the interaction between nucleons, TDSLDA suffers from a similar deficiency, an absence of a very accurate NEDF. The latest efforts to produce *ab initio* NEDF [9] lead to NEDF with quite large errors in the binding energy of nuclei, as even the most advanced *ab initio* approaches fail to accurately predict the properties of heavy nuclei yet [10]. It will take a long time until the accuracy of the phenomenological NEDFs could be matched by *ab initio* methods. In this respect the situation in nuclear physics is similar to the situation of the Standard Model (SM) of elementary particles, which still depends of a very large number of phenomenological parameters. On the other hand we can be certain that the DFT theoretical framework is otherwise correct. An accurate NEDF depends only on 7 phenomenological parameters [11], as compared with 19 in the case of SM.

4 Fission within TDSLDA

Presently, the microscopic description of fission can only cover the dynamics from the outer fission barrier until the FFs are well spatially separated. The formation of a compound nucleus and its evolution up to the outer fission barrier is a very long process, $\approx 10^{5-6}$ fm/c, too long to be numerically described microscopically with available computer capabilities within the next decade or so at least.

The goal of a fully microscopic approach to fission dynamics is to have as the only input: 1) a nuclear energy density functional (NEDF), which is fully characterized by the listed above essential nuclear ingredients; 2) the proton and neutron numbers of the compound nucleus; 3) its excitation energy and initial spin. From these ingredients alone one should be able to predict both some experimentally accessible observables as well as a number of FF properties, which are unlikely ever to be measured, but relevant for phenomenology or the origin of elements in the Universe: total kinetic energy (TKE) and the total excitation energies (TXE) of the FFs and its sharing between FFs, the FF proton and neutron numbers, FF spin and parities, FF excitation energies before the emission of neutrons and statistical gammas, the mass and charge yields, and hopefully also the correlations between various observables. Once these FF properties have been extracted they can be further used in post-processing approaches such as CGMF [22], FREYA [23] FIFRELIN [24] to further improve them and to extract neutron multiplicities and gamma spectra.

The non-equilibrium character of fission dynamics is a well established experimental fact. In induced fission $^{235}\text{U}(n_{th}, f)$ [25] one starts with relatively cold quantum

system, where pairing correlations, at the top of the outer fission barrier, are essential ingredients, as has been established by theory since 1970s. The average TKE of the FFs is $\approx 170 - 175$ MeV, while the mass difference between the compound nucleus and final products is ≈ 210 MeV. As a result the FFs end up, before emitting any prompt neutrons or gammas with roughly 40 MeV of excitation energy to share among them. Therefore, the FFs emerge hot from an initial cold compound nucleus, with the heavy FF (HFF) colder than the light FF (LLF), see also Fig. 1. The assumption that a nucleus is a mostly incompressible liquid drop, can be easily quantified within the fully quantum framework TDSLDA, for which the total energy E_{tot} is conserved. As for any liquid in motion, the total energy can be uniquely separated into two parts

$$E_{tot} = E_{int}(t) + E_{flow}(t), \quad (1)$$

$$E_{flow}(t) = \int d^3r \frac{\mathbf{j}^2(\mathbf{r}, t)}{2mn(\mathbf{r}, t)} \quad (2)$$

where $n(\mathbf{r}, t)$ is the nucleon number density, $\mathbf{j}(\mathbf{r}, t)$ is the collective momentum flow of the nuclear fluid, m the nucleon mass, and $E_{int}(t)$ the part of the nucleus energy which depends only on the matter distribution. In the only available microscopic evaluation of $E_{flow}(t)$ [18, 20] it was demonstrated that a fissioning nucleus, while descending from the top of the outer barrier on the way to the scission configuration, has an almost negligible collective flow energy of the order of 1-2 MeV, in spite of the fact that the energy difference in numerous calculated collective potential energy surfaces shows a gain of ≈ 20 MeV. The microscopic collective potential energy surfaces are evaluated by minimizing the total energy of a nucleus enforcing various in the presence of various quadrupole, octupole, hexadecapole, etc. deformation constrains [26], therefore assuming that while evolving towards scission a nucleus is always at zero intrinsic temperature. While sliding down towards scission the nuclear shape evolves very slowly, as that of an extremely viscous fluid, with a collective speed almost an order of magnitude smaller than in an adiabatic shape evolution of the nuclear shape. The nuclear shape evolution is clearly an irreversible and a highly non-equilibrium process, during which the average properties of the FFs slowly emerge, though they are not yet fully defined.

Apart from microscopically firmly establishing for the first time that the large amplitude collective motion (LACM) in fission dynamics is strongly damped it was also shown that the TKE, TXE and average FF proton and neutron numbers are predicted with a roughly 1% accuracy [17, 18, 30], without the resorting to any approximations or any unchecked theoretical assumptions, such as the introduction of collective potential energy surface and collective inertia, which assume that LACM is adiabatic, as was the prevailing attitude of theorists over several decades until now [31–33]. The strongly damped character of LACM provides the theoretical justification for the of the brownian motion model [34–37]. Phenomenologically, in order to describe the fission yields alone a plethora of models has been suggested in literature, all of them succeeding in explaining data, due to a sufficient number of

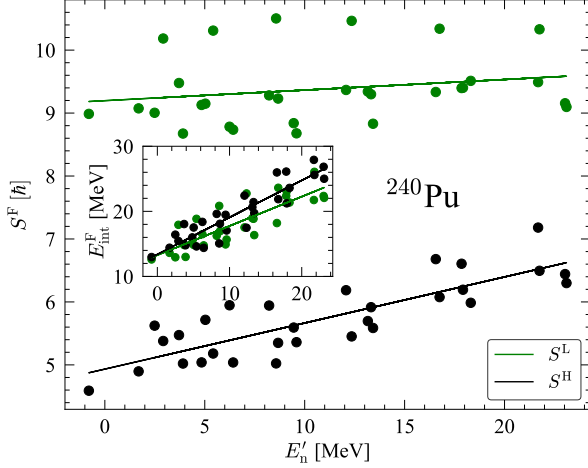


Figure 1. (Color online) The average intrinsic spins $S^{L,H}$ versus the initial FF equivalent neutron energy $E_n^* = E^* - S_n$ (E^* and S_n are the excitation energy and S_n the neutron separation energy) for the reaction $^{239}\text{Pu}(n,f)$ with SkM* NEDF. The solid lines are linear fits over the data, $S^L = 0.0168 E_n^* + 9.197$ and $S^H = 0.0732 E_n^* + 4.933$ respectively, as a function of equivalent neutron energy E_n^* along with their linear fits. In the inset we display the FF excitation energies and their linear fits $E_{\text{int}}^L = 0.4505 E_n^* + 13.25$ and $E_{\text{int}}^H = 0.5676 E_n^* + 13.40$. Using $E_{\text{int}}^F \approx A^F (T^F)^2 / 10$ [17, 27] it follows that on average $T^L > T^H$.

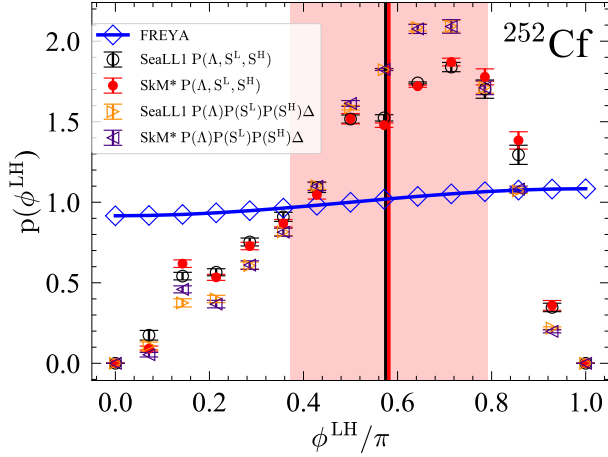


Figure 2. The circles and bullets represent the histogram (bin size = 0.22 radian) of the angle between the FF intrinsic spins S^L and S^H , extracted using the triple distribution $P(\Lambda, S^L, S^H)$ obtained in Ref. [28] and illustrated in Fig. 3 to evaluate $p(\phi^{LH})$, $\int_0^\pi d\phi^{LH} p(\phi^{LH}) = 1$. The triangles represent the histogram obtained with $P(\Lambda)P(S^L)P(S^H)\Delta$, see Ref. [28]. The blue line and diamonds are the prediction of the FREYA model [29]. The distributions $p(\phi^{LH})$ for $^{236}\text{U}^*$ and $^{240}\text{Pu}^*$ are very similar. This figure is reproduced from Ref. [28].

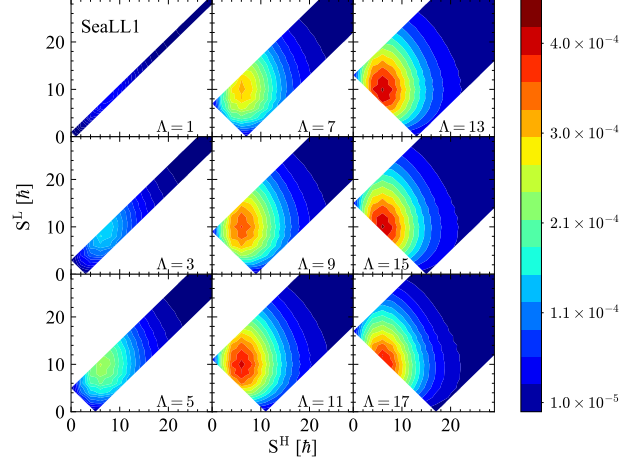


Figure 3. The ^{252}Cf triple probability distribution $P(\Lambda, S^L, S^H)$ for SeaLL1 NEDF for odd values of Λ . The FF parities are correlated with the orbital angular momentum $\pi^L \pi^H = (-1)^\Lambda$. This triple distribution vanishes outside the region $|S^L - S^H| \leq \Lambda \leq S^L + S^H$, shown with white in these plots. The distributions for $^{236}\text{U}^*$ and $^{240}\text{Pu}^*$ are very similar. This figure is reproduced from Ref. [28].

phenomenological parameters and based of contradictory theoretically unchecked assumptions [38–48] (to quote a few). The only conclusion one can draw from these approaches is that FF yields are largely insensitive to the model and their often contradictory assumptions.

Another aspect of the fission dynamics which proved rather difficult to interpret correctly is to explain how the FF intrinsic spins are generated, see the recent experimental results [49], where it was stated that the FF spins are generated after scission. The Coulomb interaction between receding FFs can lead to some contribution to the final FF spins [50, 51], but not fully explain their magnitudes, distributions, and correlations. Many other phenomenological models have been suggested over the years and the recent workshop [52] can provide some insight into the literature. While the initial spin the compound momentum nucleus is very small, and zero in case of spontaneous fission of ^{252}Cf for example, the FFs have an average spin of the order of $10\hbar$ [49, 53] with the spin of the HFF on average smaller than the spin of the LFF as established by microscopic calculations [28, 54, 55]. Fig. 1 is an example of the dependence of the FF intrinsic spins and in the inset the excitation energy of the two FFs as a function of the initial excitation energy of the compound nucleus obtained from TDSDA simulations.

While the theoretical literature addressing the FF spins is quite extensive, see references in Refs.[28, 29, 54, 55], I will discuss here only the latest phenomenological approach FREYA [29, 55–58] used to compare its predictions with recent data [49]. In FREYA the FF spins and their relative orbital angular momentum are treated classically, assuming that the rotational energy

$$E_{\text{rot}} = \frac{\mathbf{S}^L \cdot \mathbf{S}^L}{2I^L} + \frac{\mathbf{S}^H \cdot \mathbf{S}^H}{2I^H} + \frac{\mathbf{\Lambda} \cdot \mathbf{\Lambda}}{2I^R}. \quad (3)$$

It is implied in this approach that these rotational degrees of freedom are thermalized before scission, as being engulfed by the rest of the nucleon degrees of freedom, which form a thermal bath. In the case of ^{252}Cf the quantum mechanical average

$$\langle \mathbf{S}^L + \mathbf{S}^H + \mathbf{\Lambda} \rangle = \mathbf{0} \quad (4)$$

should vanish at all times. The two emerging, but not fully defined, FFs are in contact with the bath only during the time the nucleus descends from the top of the outer barrier until scission. After separation each FF is isolated and its spin is conserved and before the compound nucleus reaches the top of the outer barrier one can safely assume that no trace of an emerging FF exists. One can easily estimate the period of rotation of an emerging FF from relation between the spin, moment of inertia and its angular velocity $\hbar S^F = I^F \omega^F$ and obtain that $2\pi/\omega^F \approx 3,400$ fm/c, assuming that $S^F \approx 10$ and I^F is the moment of inertia of a rigid sphere. Therefore the period of rotation of a FF while still in contact with the other FF and the thermal bath is significantly longer than the time needed for the compound nucleus to descend from the top of the outer barrier to scission, which is $\approx 1,500$ fm/c. From numerous kinetic studies of gases it is known that starting with arbitrary initial conditions one reaches an approximate Boltzmann distribution after 3-5 collisions. A classical rigid rotor would need to arrive in equilibrium with the bath at an average angular momentum of $10\hbar$ in the time it barely performs half a rotation, thus an uncertainty in the angle $\Delta\phi \approx O(\pi)$, and therefore a wave packet with an enormous uncertainty $\Delta S \Delta\phi = O(10)$. Whether such a classical model with such large uncertainty is realistic to describe its equilibration with the rest of the nuclear system or even only of its rotational modes in such a short time, it is not obvious. Other potential issues with the assumption adopted in FREYA have been discussed in Refs. [28, 59].

So far only the phenomenological model FREYA has made a prediction concerning the angle between the spins of the two emerging FFs in Ref. [56]. Soon after that the TDSLDA microscopic treatment has also made a prediction [28], see also Ref. [59], and the two theoretical predictions are in stark disagreement with each, see Fig. 2. Several experimental groups plan to shed light on this issue (L. Sobotka private communication).

In Refs. [28, 54] we have evaluated for the first time in a fully microscopic approach the single and triple distribution of the FF intrinsic spins and their relative orbital angular momentum and also their correlations. From the triple angular momentum distribution extracted in Refs. [28, 59] one can determine the single and double FF distributions

$$P_1(S^F) = \sum_{\Lambda, f \neq F} P_3(S^F, S^f, \Lambda), \quad (5)$$

$$P_1(\Lambda) = \sum_{S^L, S^H} P_3(S^L, S^H, \Lambda), \quad (6)$$

$$P_2(S^L, S^H) = \sum_{\Lambda} P_3(S^L, S^H, \Lambda), \quad (7)$$

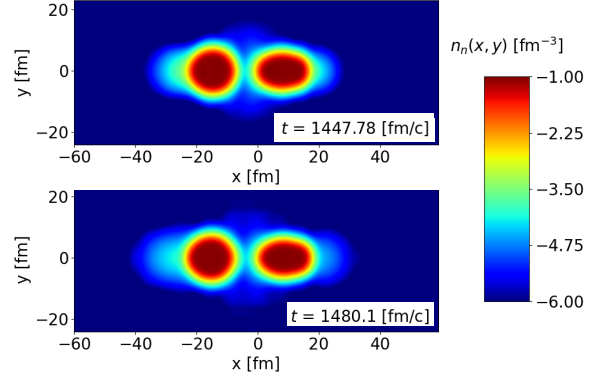


Figure 4. Two consecutive frames of the neutron distribution after the two FFs separated in $^{235}\text{U}(n,f)$ induced fission. The HFF is on the left and the LFF is on the right and the yellow band is the surface of each fragment, where the neutron number density is $< 0.01 \text{ fm}^{-3}$. While one can clearly see some neutrons emitted from the neck, most neutrons appear to be emitted in the direction of the motion of each FF. (The colorbar shows the $\log n_n$.)

and evaluate

$$\sum_{S^L, S^H, \Lambda} |\mathcal{N} P(\Lambda) P_1(S^L) P_1(S^H) \Delta - P_3(S^L, S^H, \Lambda)| = 0.35, \quad (8)$$

$$\sum_{S^L, S^H} |P_2(S^L, S^H) - P_1(S^L) P_1(S^H)| = 0.02, \quad (9)$$

where \mathcal{N} is a normalization constant and Δ enforces Eq. (4). Eq. (8) reveals that the two FF spins and the relative orbital angular momentum are rather strongly correlated. At the same time, Eq. (9) tells us that if one measure $P_2(S^L, S^H)$ the two FF spins appear practically uncorrelated, as observed in the recent experiment [49]. This is in stark contradiction with the assertion made by Wilson *et al.* [49], and who interpreted this absence of correlations between the two FF spins as an argument that these spins are generated after the FFs are separated. The FFs emerge very deformed after scission, and their shapes relax significantly after scission [17, 18], however the total wave function of the entire system is strongly correlated and the two emerging FFs are entangled, see also below. The presence of an “angular momentum bath Λ ” appear to be sufficient to ensure the apparent independence of the two FF spins, in spite of the triple strong FF correlations with Λ .

Since we follow the two FFs until they are widely separated we can get insight into the neutron emission before the FFs are fully accelerated. There is a long debate in literature concerning the existence of scission neutrons and, more specifically neutrons emitted from the neck forming between the two emerging fragments before scission, see references in Ref. [60]. While the FFs are being accelerated the mean field potential experienced by neutrons is tilted, as in a bucket filled with water, and neutrons can escape. In Fig. 4 we show the neutron number density profile

at two instances after scission. One can see the formation of neutron clouds in front of both FFs neutrons, along the fission axis. At the same time there are neutrons emitted perpendicular to the fission axis, in the region between the two FFs, which might be considered to be emitted from the “neck.” As these results are still being analyzed and we did not accumulate enough data yet, and we are not prepared yet to provide more detailed estimates concerning the number and spectrum of these emitted neutrons.

What happens to the FF shapes after scission, apart from the fact the the FFs recede very fast from one another due to Coulomb repulsion? This is an aspect which is not incorporated in any phenomenological FF yields studies, even though often it is recognized, but almost never correctly quantified that the FFs relax their shapes. In Refs. [17, 18] it was also demonstrated that the FF shapes continue to evolve in the same manner as before the scission, very slowly and irreversibly, and deformation energy is converted into internal excitation energy (thermal). While this stage is relatively slow, it is also many order of magnitude shorter that the time scale an emerging FF starts emitting prompt neutrons and statistical gammas. In Fig. 5 one can see the neutron multiplicity spectrum obtained using the Hauser-Feshbach framework [22] with input from TDSLDA is a significant improvement over what the default phenomenological GCMF predicted so far.

5 High-momentum tails, entanglement entropy

The TDSLDA simulations of fission are performed on a spatial cartesian lattice, with a lattice constant $l = 1$ fm, which corresponds to a momentum cutoff [62] $p_{cut} = \hbar\pi/l \approx 600$ MeV/c. This value of the momentum cutoff is on the upper limit considered in extracting the nucleon interactions within the χ Effective Field Theory, and one might expect that (some) short range correlations (SRCs) are present within TDSLDA. Indeed, as discussed in Refs. [61, 63, 64] nn and pp SRCs are indeed present and as expected they show up in the single-particle momentum distribution, see Fig. 6, where at momenta larger than the Fermi momentum one clearly observes that $n_k = C/k^4$, where k is the wave vector and C is Tan contact [65–68]. Such a behavior of n_k has been predicted also by Sartor and Mahaux [69] and put in evidence in experiments at the Jefferson National Laboratory [70, 71]. In nuclei np correlations, in particular the tensor np interaction, are the dominant source of the behavior $n_k = C/k^4$, which are absent in TDSLDA, but which we plan to include the generalized TDSLDA [63]. The n_k long momentum tails shown in Fig. 6 are present at all times and all excitation energies, in particular in the fully separated FFs, when pairing correlations are absent. In order to evaluate the momentum distribution shown in Fig. 6 one has to find the eigenfunction and eigenvalues of the one-body density matrix $n(\xi, \zeta)$, known as canonical wave functions in superconductivity/superfluidity [31] and natural orbitals, mainly in chemistry and lately also in nuclear physics [72–

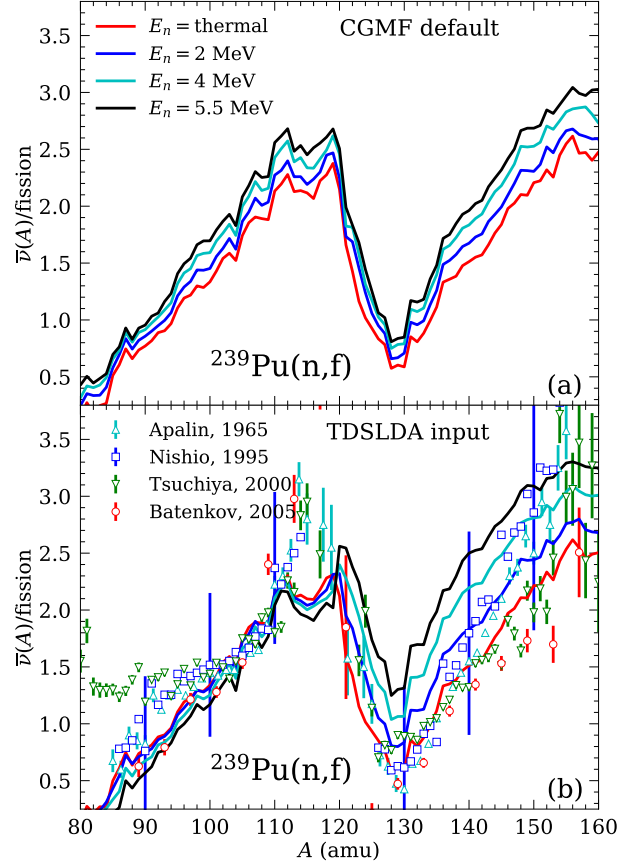


Figure 5. We compare in Ref. [17] the average prompt neutron multiplicity $\bar{\nu}(A)$ emitted by FFs in the case of a default CGMF simulation [22], which assumes no E_n dependence for the energy sharing, with the one extracted using the the excitation energy sharing between the FFs in our calculation with NEDF SeaLL1, as a function of the equivalent incident neutron energy in $^{239}\text{Pu}(n,f)$ reaction along with available experimental data for the reaction $^{239}\text{Pu}(n_{th},f)$ from various experiments. The fragment mass A is before neutron emission. In the GCMF default version the effect of the incident neutron energy is significantly milder that when TDSLDA input is used, which leads to better agreement with data.

75],

$$n(\xi, \zeta) = \langle \Phi | \psi^\dagger(\zeta) \psi(\xi) | \Phi \rangle, \quad (10)$$

$$\int d\zeta n(\xi, \zeta) \phi_k(\zeta) = n_k \phi_k(\xi), \quad 0 \leq n_k \leq 1, \quad (11)$$

where $\xi = (\mathbf{r}, \sigma, \tau)$, $\zeta = (\mathbf{r}', \sigma', \tau')$ are the spatial, spin, and isospin coordinates. The rather unexpected and surprising lesson emerging from these results is that within TDSLDA one can describe both long-range and short-range correlations. This a long-time dream in theoretical physics, to generate a formalism which includes apart from the mean field evolution, as in TDHF, also the effect of collisions, as in the semiclassical Boltzmann-Uehling-Uhlenbeck (BUU) equation [76, 77]. The BUU equation is semiclassical in character, and similarly to TDDFT, is an equation for the one-body density, even though it goes well beyond mean field, but it depends on probabilities, a typical feature of classical descriptions. A quantum approach should depend on amplitudes in order to describe interfer-

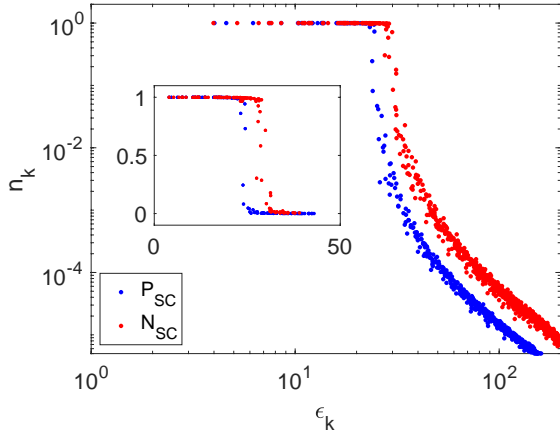


Figure 6. The canonical occupation probability n_k as a function of $\epsilon_k = \langle \phi_k | -\hbar^2 \Delta / 2m | \phi_k \rangle$. In the inset we show that the canonical occupation probabilities n_k around the Fermi level have the expected textbook behavior. Notice the presence of SRCs for $\epsilon_k \propto 1/k^4 > 120$ MeV. This figure is from Ref. [61]

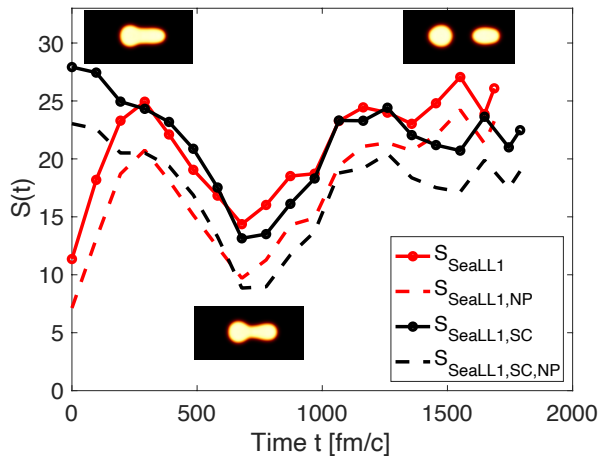


Figure 7. The time-dependence of the entropy $S(t)$ evaluated in the case of the induced fission of $^{235}\text{U}(n,f)$ with a low energy neutron as a function of time from the vicinity of the outer saddle point until the two fission fragments are fully separated. The solid curves correspond are entanglement entropies evaluated without particle projection of the total many-body wavefunction, while the dashed curves are obtained after particle projection was performed before the canonical occupation probabilities were evaluated. (For red curves see Ref. [61].) The nuclear shapes obtained in TDSLDA during the time evolution are shown at 0, 675, and 1650 fm/c, from Ref. [61].

ence, quantized vortices, quantum turbulence, and entanglement, and the generalized TDSLDA is such a framework [63].

A still unresolved problem in theoretical physics is how to characterize the complexity of a many-body wave function. The simplest many-body wave function for fermions is a Slater determinant and the introduction of correlations leads to many-body wave functions which are sums of many Slater determinants, as in the case of shell-model calculations, where the size of the Hilbert space can

reach billions [75]. However, the number of Slater determinants in an expansion of a many-body wave function depends exponentially on the size and type of the single-particle basis used and a characterization of the complexity a many-body wave function by the dimensionality of the many-body Hilbert space is thus ill-defined. However, the complexity can be quantified for any quantum state $|\Phi\rangle$ by evaluating the orbital entanglement/quantum Boltzmann entropy [63, 76–82]

$$S = -g \sum_k n_k \ln n_k - g \sum_k [1 - n_k] \ln [1 - n_k], \quad (12)$$

where g is the spin-isospin degeneracy, \sum implies summation over discrete and integral over continuous variables and n_k are the canonical occupation probabilities. This orbital entanglement entropy vanishes for a Slater determinant and is positive for any other many-body wave function and reaches its maximum value when all n_k are equal to each other. In the limit of a dilute and weakly interacting system this entanglement entropy approaches the quantum Boltzmann entropy of that many-fermion system. Since the set and the values of the canonical occupation probabilities are independent of the single-particle basis used it also allows for a unique definition of the orbital entanglement entropy, which can be used to characterize the complexity of the many-body wave function. In the case of a dilute and weakly interacting many-fermion system $S(t)$ as a function of time can only increase, $\dot{S}(t) \geq 0$. For a strongly interacting system however the time dependence of $S(t)$ is more complicated [83, 84] and the question, what can we learn from it. Clearly the orbital entanglement entropy $S(t)$ gives us unique measure on how complicated the many-body wave function is at any time during its evolution. $-\ln n_k$ are known in literature as the entanglement spectrum [85], play in particular an important role in gauge theories and condensed matter [85, 86] and carry more detailed information about the many-body system than the single number $S(t)$.

We have extracted $S(t)$ in the case of $^{235}\text{U}(n,f)$ for both particle unprojected and particle projected many-nucleon wave functions within TDSLDA, see Fig. 7. After particle projection the nuclear many-body wave function is a sum over an exponentially large number of Slater determinants with fixed N and Z numbers, thus indeed a very complex function. While a fissioning nucleus evolves from the top of the outer barrier it develops a neck, which hinders the particle exchange between the two halves of the system. Immediately after scission however the two FFs are highly excited, strongly entangled, and mostly isolated apart from the long-range Coulomb interaction between them. Their shapes still evolve in time and the two FFs evolve towards their individual thermal equilibrium and $\dot{S}(t) > 0$ as expected, due to the presence of nn and pp collisions, which lead to the long momentum tails $n_k = C/k^4$. For more details see Refs. [61, 63, 64].

6 Conclusions

The only input needed to extract information about the fission dynamics is encoded in only seven parameters,

which define the nuclear energy density functional for both stationary and time-dependent phenomena and which are known with good accuracy for decades. Within the TD-SLDA description of fission we have shown that the nuclear large amplitude collective motion is strongly dissipative, extracted TKE, TXE, average FF proton and neutron, have shown how the excitation energy is shared between FFs and how it depends on the excitation energy of the compound nucleus, the evolution of the FF shapes after scission, evaluated the FF spin distribution and their correlations, have insight into the character of the neutrons emitted immediately after scission, but before the FFs are fully accelerated, described the prompt neutron multiplicity and their dependence on the energy of the compound nucleus, and evaluated the entanglement entropy, which sheds an unparalleled light on the complexity of the time-dependent many-body wave function of a fissioning nucleus and on how its complexity evolves with time. This time-dependent microscopic approach has a strong predictive power, without any assumptions and uncontrolled approximations and fitting parameters, has already helped guide and improve phenomenological models, delivers accurate and comprehensive information, and predicts properties which are not accessible in the laboratory, and likely will play an important role in helping elucidate the origin of elements, which are formed through fission of nuclei which are not possible to study experimentally.

The fission results presented here have been obtained since 2016 in collaboration with I. Stetcu, S. Jin, I. Abdurrahman, K. Godbey, K.J. Roche, P. Magierski, and N. Schunck. The funding from the US DOE, Office of Science, Grant No. DE-FG02-97ER41014 and also the support provided in part by NNSA cooperative Agreement DE-NA0003841 is greatly appreciated. This research used resources of the Oak Ridge Leadership Computing Facility, which is a U.S. DOE Office of Science User Facility supported under Contract No. DE-AC05-00OR22725.

References

- [1] O. Hahn, F. Strassmann, *Naturwissenschaften* **27**, 11 (1939)
- [2] L. Meitner, L., O.R. Frisch, *Nature* **143**, 239 (1939)
- [3] P. Hohenberg, W. Kohn, *Phys. Rev.* **136**, B864 (1964)
- [4] W. Kohn, L.J. Sham, *Phys. Rev.* **140**, A1133 (1965)
- [5] E. Runge, E.K.U. Gross, *Phys. Rev. Lett.* **52**, 997 (1984)
- [6] R.M. Dreizler, E.K.U. Gross, *Density Functional Theory: An Approach to the Quantum Many-Body Problem* (Springer-Verlag, Berlin, 1990), ISBN 9780387519937
- [7] M.A.L. Marques, C.A. Ullrich, F. Nogueira, A. Rubio, K. Burke, E.K.U. Gross, eds., *Time-Dependent Density Functional Theory*, Vol. 706 of *Lecture Notes in Physics* (Springer-Verlag, Berlin, 2006), ISBN 978-3-540-35422-2
- [8] M.A.L. Marques, N.T. Maitra, F.M.S. Nogueira, E.K.U. Gross, A. Rubio, eds., *Fundamentals of Time-Dependent Density Functional Theory*, Vol. 837 of *Lecture Notes in Physics* (Springer, Heidelberg, 2012)
- [9] F. Marino, C. Barbieri, A. Carbone, G. Colò, A. Lovato, F. Pederiva, X. Roca-Maza, E. Vigezzi, *Phys. Rev. C* **104**, 024315 (2021)
- [10] B. Hu, W. Jiang, T. Miyagi, Z. Sun, A. Ekström, C. Forssén, G. Hagen, J.D. Holt, T. Papenbrock, S.R. Stroberg et al., *Nature Physics* **18**, 1196 (2022)
- [11] A. Bulgac, M.M. Forbes, S. Jin, R.N. Perez, N. Schunck, *Phys. Rev. C* **97**, 044313 (2018)
- [12] M. Brack, J. Damgaard, A.S. Jensen, H.C. Pauli, V.M. Strutinsky, C.Y. Wong, *Rev. Mod. Phys.* **44**, 320 (1972)
- [13] S. Bjornholm, J. Lynn, *Rev. Mod. Phys.* **52**, 725 (1980)
- [14] G. Bertsch, *Phys. Lett. B* **95**, 157 (1980)
- [15] G.F. Bertsch, A. Bulgac, *Phys. Rev. Lett.* **79**, 3539 (1997)
- [16] G.F. Bertsch, *Int. J. Mod. Phys.* **26**, 1740001 (2017)
- [17] A. Bulgac, S. Jin, K.J. Roche, N. Schunck, I. Stetcu, *Phys. Rev. C* **100**, 034615 (2019)
- [18] A. Bulgac, S. Jin, I. Stetcu, *Frontiers in Physics* **8**, 63 (2020)
- [19] A. Bulgac, *Ann. Rev. Nucl. and Part. Sci.* **63**, 97 (2013)
- [20] A. Bulgac, *Physica Status Solidi B* **2019**, 1800592 (2019)
- [21] N. Bohr, J.A. Wheeler, *Phys. Rev.* **56**, 426 (1939)
- [22] B. Becker, P. Talou, T. Kawano, Y. Danon, I. Stetcu, *Phys. Rev. C* **87**, 014617 (2013)
- [23] R. Vogt, J. Randrup, J. Pruet, W. Younes, *Phys. Rev. C* **80**, 044611 (2009)
- [24] O. Litaize, O. Serot, D. Regnier, S. Theveny, S. Onde, *Physics Procedia* **31**, 51 (2012)
- [25] D. Madland, *Nucl. Phys. A* **772**, 113 (2006)
- [26] P. Marević, N. Schunck, E. Ney, R. Navarro Pérez, M. Verriere, J. O'Neal, *Computer Physics Communications* **276**, 108367 (2022)
- [27] A. Bohr, B.R. Mottelson, *Nuclear Structure*, Vol. I (Benjamin Inc., New York, 1969), ISBN 9810231970
- [28] A. Bulgac, I. Abdurrahman, K. Godbey, I. Stetcu, *Phys. Rev. Lett.* **128**, 022501 (2022)
- [29] J. Randrup, R. Vogt, *Phys. Rev. Lett.* **127**, 062502 (2021)
- [30] A. Bulgac, P. Magierski, K.J. Roche, I. Stetcu, *Phys. Rev. Lett.* **116**, 122504 (2016)
- [31] P. Ring, P. Schuck, *The Nuclear Many-Body Problem*, Number 17 in *Theoretical and Mathematical Physics Series*, 1st edn. (Springer-Verlag, Berlin Heidelberg New York, 2004), ISBN 978-3-540-21206-5
- [32] N. Schunck, L.M. Robledo, *Rep. Prog. Phys.* **79**, 116301 (2016)
- [33] J.K. Krappe, K. Pomorski, *Theory of Nuclear Fission* (Springer Heidelberg, 2012)
- [34] D.E. Ward, B.G. Carlsson, T. Døssing, P. Möller, J. Randrup, S. Åberg, *Phys. Rev. C* **95**, 024618

- (2017)
- [35] M. Albertsson, B. Carlsson, T. Døssing, P. Möller, J. Randrup, S. Åberg, *Physics Letters B* **803**, 135276 (2020)
- [36] M. Albertsson, B.G. Carlsson, T. Døssing, P. Möller, J. Randrup, S. Åberg, *Phys. Rev. C* **103**, 014609 (2021)
- [37] M. Albertsson, B.G. Carlsson, T. Døssing, P. Möller, J. Randrup, S. Åberg, *Phys. Rev. C* **104**, 064616 (2021)
- [38] B.D. Wilkins, E.P. Steinberg, R.R. Chasman, *Phys. Rev. C* **14**, 1832 (1976)
- [39] J. Randrup, P. Möller, *Phys. Rev. Lett.* **106**, 132503 (2011)
- [40] Y. Aritomo, S. Chiba, F. Ivanyuk, *Phys. Rev. C* **90**, 054609 (2014)
- [41] A.J. Sierk, *Phys. Rev. C* **96**, 034603 (2017)
- [42] C. Ishizuka, M.D. Usang, F.A. Ivanyuk, J.A. Maruhn, K. Nishio, S. Chiba, *Phys. Rev. C* **96**, 064616 (2017)
- [43] J. Sadhukhan, W. Nazarewicz, N. Schunck, *Phys. Rev. C* **93**, 011304 (2016)
- [44] J. Sadhukhan, C. Zhang, W. Nazarewicz, N. Schunck, *Phys. Rev. C* **96**, 061301 (2017)
- [45] D. Regnier, N. Dubray, N. Schunck, M. Verrière, *Phys. Rev. C* **93**, 054611 (2016)
- [46] D. Regnier, N. Dubray, N. Schunck, *Phys. Rev. C* **99**, 024611 (2019)
- [47] J.F. Lemaître, S. Panebianco, J.L. Sida, S. Hilaire, S. Heinrich, *Phys. Rev. C* **92**, 034617 (2015)
- [48] J.F. Lemaître, S. Goriely, A. Bauswein, H.T. Janka, *Phys. Rev. C* **103**, 025806 (2021)
- [49] J.N. Wilson, *et al.*, *Nature* **590**, 566 (2021)
- [50] G.F. Bertsch, *Reorientation in newly formed fission fragments* (2019), 1901.00928
- [51] G. Scamps, *Microscopic description of the torque acting on fission fragments* (2022), 2209.10759
- [52] *Workshop on Fission Fragment Angular Momenta, Seattle, USA, June 21-24, (2022)*, <https://indico.in2p3.fr/event/26459/> (???), <https://indico.in2p3.fr/event/26459/>
- [53] J.B. Wilhelmy, E. Cheifetz, R.C. Jared, S.G. Thompson, H.R. Bowman, J.O. Rasmussen, *Phys. Rev. C* **5**, 2041 (1972)
- [54] A. Bulgac, I. Abdurrahman, S. Jin, K. Godbey, N. Schunck, I. Stetcu, *Phys. Rev. Lett.* **126**, 142502 (2021)
- [55] P. Marević, N. Schunck, J. Randrup, R. Vogt, *Phys. Rev. C* **104**, L021601 (2021)
- [56] R. Vogt, J. Randrup, *Phys. Rev. C* **103**, 014610 (2021)
- [57] J. Randrup, T. Døssing, R. Vogt, *Phys. Rev. C* **106**, 014609 (2022)
- [58] J. Randrup, *Phys. Rev. C* **106**, L051601 (2022)
- [59] A. Bulgac, *Phys. Rev. C* **106**, 014624 (2022)
- [60] A. Bulgac, *Phys. Rev. C* **102**, 034612 (2020)
- [61] A. Bulgac, M. Kafker, I. Abdurrahman, *Measures of complexity and entanglement in fermionic many-body systems* (2022), 2203.04843
- [62] A. Bulgac, M.M. Forbes, *Phys. Rev. C* **87**, 051301(R) (2013)
- [63] A. Bulgac, *Phys. Rev. C* **105**, L021601 (2022)
- [64] A. Bulgac, *Entanglement entropy, single-particle occupation probabilities, and short-range correlations* (2022), 2203.12079
- [65] S. Tan, *Ann. Phys.* **323**, 2952 (2008)
- [66] S. Tan, *Ann. Phys.* **323**, 2971 (2008)
- [67] S. Tan, *Ann. Phys.* **323**, 2987 (2008)
- [68] W. Zwerger, ed., *The BCS–BEC Crossover and the Unitary Fermi Gas*, Vol. 836 of *Lecture Notes in Physics* (Springer-Verlag, Berlin Heidelberg, 2012)
- [69] R. Sartor, C. Mahaux, *Phys. Rev. C* **21**, 1546 (1980)
- [70] O. Hen et al., *Science* **346**, 614 (2014)
- [71] O. Hen, G.A. Miller, E. Piaseczky, L.B. Weinstein, *Rev. Mod. Phys.* **89**, 045002 (2017)
- [72] P.O. Löwdin, *Phys. Rev.* **97**, 1474 (1955)
- [73] A.J. Coleman, *Rev. Mod. Phys.* **35**, 668 (1963)
- [74] E.R. Davidson, *Rev. Mod. Phys.* **44**, 451 (1972)
- [75] C.W. Johnson, *Current Status of Very-Large-Basis Hamiltonian Diagonalizations for Nuclear Physics* (2018), 1809.07869
- [76] L.W. Nordheim, *Proc. Roy. Soc. (London)* **A119**, 689 (1928)
- [77] E.A. Uehling, G.E. Uhlenbeck, *Phys. Rev.* **43**, 552 (1933)
- [78] R. Horodecki, P. Horodecki, M. Horodecki, K. Horodecki, *Rev. Mod. Phys.* **81**, 865 (2009)
- [79] M. Haque, O.S. Zozulya, K. Schouten, *J. Phys. A Math. Theor.* **42**, 504012 (2009)
- [80] J. Eisert, M. Cramer, M.B. Plenio, *Rev. Mod. Phys.* **82**, 277 (2010)
- [81] K. Boguslawski, P. Tecmer, *Int. J. Quant. Chem.* **115**, 1289 (2014)
- [82] C. Robin, M.J. Savage, N. Pillet, *Phys. Rev. C* **103**, 034325 (2021)
- [83] A. Del Maestro, H. Barghathi, B. Rosenow, *Phys. Rev. B* **104**, 195101 (2021)
- [84] A. Del Maestro, H. Barghathi, B. Rosenow, *Phys. Rev. Research* **4**, L022023 (2022)
- [85] H. Li, F.D.M. Haldane, *Phys. Rev. Lett.* **101**, 010504 (2008)
- [86] N. Mueller, T.V. Zache, R. Ott, *Phys. Rev. Lett.* **129**, 011601 (2022)